RSC Advances




ROYAL SOCIETY OF CHEMISTRY

www.rsc.org/advances

RSC Advances RSCPublishing

ARTICLE

# Largely reinforced polyurethane via simultaneous incorporation of poly (lactic acid) and multiwalled carbon nanotubes

Cite this: DOI: 10.1039/x0xx00000x

Received 00th January 2015,
Accepted 00th January 2015

DOI: 10.1039/x0xx00000x

www.rsc.org/

Yan Zhou, Hao Xiu, Jia Dai, Hongwei Bai, Qin Zhang and Qiang Fu*

In this study, we simultaneously introduced both poly(lactic acid) (PLA) and multiwalled carbon nanotubes (CNTs) into the polyurethane (PU) matrix via melt blending, to achieve a balanced mechanical properties and good conductivity. Different contents of PLA (0-30 *wt*.%) and CNTs( 0-3.0 *wt*.%) were used in this work. A significant improvements of tensile strength at 300% strain and Young's modulus were observed, which could not be obtained by incorporating either PLA or CNTs with PU separately. Particularly, the ternary composites containing a large amount of PLA (30 *wt*.%), 70PU/30PLA/CNTs composites, exhibit superior mechanical properties compared to other composites with less PLA content but the same amounts of CNTs. Moreover, the ternary composites showed better electrical conductivity compared with the binary counterpart. SEM observations demonstrated that PLA particles and CNTs are separately dispersed in PU matrix. It was found that PLA particles remain spherical and its size increases with increasing of PLA content up to 30*wt*.%, while a network structure of CNTs is formed with increasing of its content, which was also confirmed via dynamic rheological analysis. Interestingly, some CNTs were seen to be located in the interfaces between PLA particles and PU matrix for 70PU/30PLA/CNTs composites, namely, some CNTs exhibit the nano-bridge effect between PU and PLA. We hypothesized that the nano-bridge structure of CNTs in the composites could mainly contribute to the observed enhancement of mechanical properties and electrical conductivity.

## 1. Introduction

Polyurethane, which contains numerous urethane groups (–HN–COO–), has attracted much attention in recent years due to its good process ability, good biocompatibility and excellent physical properties including elasticity, abrasion resistance, flexibility, durability, and toughness[1-5]. Its many uses range from rigid foam to flexible foam[6], appliances from thermoplastic polyurethane used in footwear, to elastomers used on automotive interiors[7-9]. However, the defects of PU, especially its low mechanical strength, have limited its applications[10-15]. Thus, it is very necessary to develop reinforced PU for wider applications.

A practical and economic strategy to reinforce PU is blending it with other polymers, for instance, ultra high molecular weight polyethylene (UHMWPE)[16], polylactic acid (PLA)[17], polycaprolactone (PCL)[18] and polyamide (PA)[19, 20] have been used to modify PU. However, the improvement in mechanical strength is not satisfying, and the elongation at break of the blends always shows a dramatic degradation. For example, in the study by Chen et al.[18], a little increase in tensile strength was realized from 0.27 MPa for neat PU to 1.69 MPa for its blend with PCL, while the elongation of the blend is reduced from 103% to 3.3% drastically. Wang et al.[16] also observed a similar elongation decrease in the system of PU/UHMWPE. Besides the blending with other polymers, another efficient method to reinforce PU is to mix with inorganic and organic fillers with high stiffiness, such as carbon nanotubes (CNTs)[21-24], functionalized graphene sheet (FGS)[25], nanosilica[26], glass fibres[27], microcrystalline cellulose[28-30] and organoclay[31]. However, due to the agglomeration of fillers during processing, these composites often show a poor flexibility at high fillers concentrations. Nguyen et al.[25] found that the tensile strength and Young's modulus of the resultant PU are almost unchanged with the incorporation of 7*wt*.% functionalized graphene sheet (FGS), while the elongation at break shows an unexpected degradation from 814% to 245%. In the study by Cotgreave et al.[27], a similar elongation decrease in the composites of PU/high-modulus chopped fibres was noticed.

The above methods demonstrate the difficulty to significantly reinforce PU by blending with either polymers or fillers separately, for which the degree of the reinforcement is usually very small and the significant decreases of elongation at break could not be avoid. It is of extreme importance to reinforce PU without damaging its ductility. It has been reported that with the simultaneously incorporation of PLA and CNTs into poly(propylene carbonate), the tensile strength and Young's modulus of PPC were increased more than one order of magnitude, and the high elongation at break was maintained[32]. Accordingly, it's logical to ask whether superior mechanical reinforcement of PU can be realized while its ductility is well maintained by simultaneously incorporating polymers and fillers into PU. Therefore, in the present study, we attempted to enhance the mechanical performance of PU without damaging its ductility by the simultaneous incorporation of poly (lactic acid) (PLA) and multiwalled carbon nanotubes (CNTs). As known, PLA is a biodegradable polymer made by converting starch or sugar produced from wheat, corn, vegetable and other biomass resources[33-35]; and it is now a widely used material due to its good mechanical strength and stiffness, which makes it an attractive option to reinforce PU[36]. Besides, CNTs is a kind of prominent modifiers for polymeric materials due to its excellent mechanical and physical properties such as high Young's modulus, high tensile strength, high aspect ratio and excellent electrical conductivity[37-42]. Thus an overall excellent mechanical and electrical performance of PU/PLA/CNTs ternary composites with wider applications could be expected. In this study, several composites with different weight ratios of PU, PLA and CNTs were designed and obtained by melt blending. It was found that the simultaneously incorporation of PLA and CNTs induces a great improvement of mechanical strength and electrical conductivities of PU. Notably, the 70PU/30PLA/CNTs composite exhibits superior mechanical properties compared to other composites with the same amount of CNTs. The synergistic effect of PLA and CNTs on the enhancement of PU was discussed based on the location and structure of and PLA and CNTs in the composites as observed via SEM or deduced from rheological analysis.

## 2. Experimental

### 2.1. Materials

Polyurethane (PU， WHT-1570) with a density of 1.21 g/cm$^3$was purchased from Yantai Wanhua Polyurethanes Co. Ltd., China. Polylactic acid (PLA，4032D, D-isomer content = 1.2-1.6%), was purchased from NatureWorks Co. Ltd., USA. Multiwall carbon nanotubes (CNTs, Nanocyl 7000，a diameter of 10 nm, length of 1.5 μm, and a surface area of 250 – 300 m$^2$/g) were kindly provided by Nanocyl S.A., Belgium, and used with no more surface modification.

### 2.2. Composites preparation

PU/PLA/CNTs (w/w/x) ternary composites with various contents of PLA(0-30 *wt.*%) and CNTs(0~3 *wt.*%) were prepared by melt compounding in a HAAKE torque rheometer (Rheomix 600, USA) at a rotor speed of 50 rpm for 10 min and the processing temperature was kept at 180℃ to ensure that PU would not decompose. Before melt blending, PU, PLA and CNTs were dried at 50℃, 50℃ and 80℃ respectively for 24 h in a vacuum oven. The obtained PU/PLA/CNTs composites were named according to the contents of PU, PLA and CNTs, for example, 70PU/30PLA/1CNTs means a composite contains 70 *wt.*% of PU, 30 *wt.*% of PLA and 1 *wt.*% of CNTs, respectively. Meanwhile, PU/PLA blends or PU/CNT composites with different weight ratio were also prepared in the same way for comparison. Specimens for further mechanical and electrical measurements were processed by compression molding at 180℃ for 5 min under a pressure of 5 MPa.

### 2.3. Characterization

**Tensile measurements:** The tensile properties were evaluated using an Instron 4302 universal tensile testing machine with a crosshead speed of 50 mm/min. The testing was carried out at room temperature (23℃) and the final results reported were the average of those measured from four to six specimens for each sample.

**Conductivity testing:** The electric resistance of the composites was measured with a Keithley 6487 picoammeter. Specimens with the size of 20 mm×6 mm×1 mm were obtained from the compression molded samples, followed with silver paint coating on both ends of the specimens to eliminate contact resistance.

**Scanning Electron Microscopy:** The phase morphologies of fractured surface of the composites were characterized by examining along their fractured edges with a field emission-scanning electron microscope (FESEM) (Inspect F, FEI, USA) at 20 kV accelerating voltage. Before the examination, the cryogenically fractured surfaces of samples were sputter-coated with a thin layer of gold. In order to investigate the dispersion state of CNTs and PLA, the cryogenically fractured surface was etched in chloroform for 10 min at room temperature to partially remove PLA.

**Dynamic rheological analysis:** The rheological properties were performed on a strain-controlled dynamic rheometer (Bohlin Gemini 2000, Malvern, British) using parallel plate with the diameter of 25mm at 190 ℃ under nitrogen atmosphere to avoid thermo-oxidative degradation. And the frequency sweep was adopted with the range of 0.01 to 100 Hz.

## 3. Results and discussion

### 3.1. Mechanical properties of PU/PLA/CNTs composites

In this study, we first investigated the mechanical properties of PU/PLA/CNTs composites with different weight ratios at room temperature. Taking as example, the stress-strain curves for the neat PU, PU/2CNTs composite, 70PU/30PLA blend and 70PU/30PLA/2CNTs composite are shown in Fig. 1. The mechanical properties for rubbers, plastics and fibres are usually



 

characterized by the tensile strength at 300% strain, yield strength and tensile strength at break, respectively. In our work, the final tensile strength at break is more or less the same for all the samples in Fig. 1. However, the improvement of tensile strength at 300% strain and Young's modulus is indeed obvious for the ternary system compared with the binary system. One observes a slight increase of tensile strength at 300% strain and modulus of PU by adding 2 *wt.*% of CNTs and also a good elongation as same as that of PU(PU/2CNTs). Again a slight increase of tensile strength at 300% strain and modulus of PU is observed by adding 30 *wt.*% of PLA, but companying with a big decrease of elongation(70PU/30PLA). For 70PU/30PLA/2CNTs composite, it is very interesting to see a large enhancement of tensile strength and modulus of PU by adding both PLA( 30 *wt.*%) and CNTs(2 *wt.*%) while maintaining the similar elongation as that of 70PU/30PLA composite.

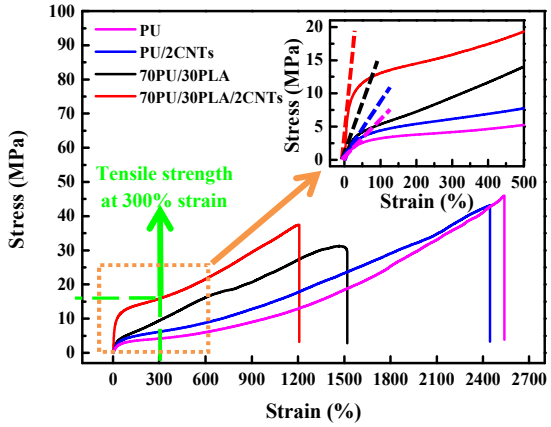


**Fig. 1.** Comparison of mechanical properties for neat PU, PU/2CNTs composite, 70PU/30PLA composite and 70PU/30PLA/2CNTs composite. The tensile test is carried out at room temperature and the stress–strain curves are partially enlarged in the inset, where the young's modulus is shown as the slope.

Typically, Fig.2 shows the effects of respective PLA and CNTs on the mechanical properties of PU. It is observed clearly from the red curve of Fig. 2-a and 2-b that PLA can improve the tensile strength of PU, while with the increasing amount of PLA, the ductility shows a dramatic degradation. For instance, when the amount of PLA is 10 *wt.*%, the tensile strength at 300% strain for the PU/PLA blends is enhanced slightly (from 4.33 MPa to 5.14 MPa) and the elongation at break shows a slight decrease. When the amount of the PLA is 20 *wt.*%, the tensile strength at 300% strain continues to increase, while the elongation at break of the composite shows a degradation from 2555 % to 2017%, and it decreases to 1600% with further addition of 30 *wt.*% PLA. The influence of CNTs on neat PU was also investigated as shown in the black curve of Fig. 2a and Fig. 2b. The tensile strength at 300% strain of the PU/CNTs composites increases from 4.33 MPa to 6.43 MPa as the content of CNTs is increased from 0 to 2 *wt.*%; meanwhile, the elongation at break shows a slight decrease from 2555% to 2373%. When 3 *wt.*% CNTs is introduced, the tensile strength at 300% strain is almost unchanged (6.54MPa) compared with the PU/2CNTs composite, while there is a further degradation in the elongation at break (2260%), which might due to the agglomeration of CNTs.

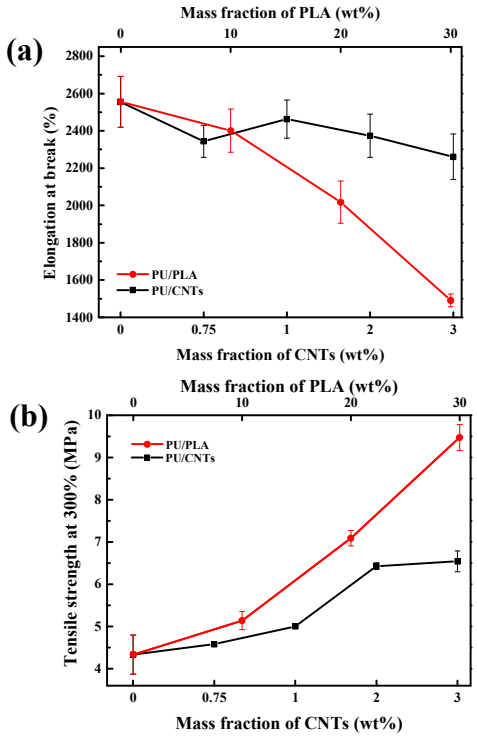


**Fig. 2.** The effects of PLA or CNTs on mechanical properties of PU.

We further investigated the mechanical properties of the PU/PLA/CNTs composites and Fig. 3 shows the results. Upon the incorporation of various contents of PLA and CNTs simultaneously, significant reinforcement in both the strength and the modulus is obtained without dramatic decreases of elongation at break of the composites compared with PU/PLA blends. As shown, the tensile strength at 300% strain increases from 4.33 MPa for the neat PU to 6.57 MPa and 14.52 MPa for the 90PU/10PLA/0.75CNTs composite and the 70PU/30PLA/0.75CNTs composite, respectively. Meanwhile, the Young's modulus of the 90PU/10PLA/0.75CNTs composite is 2.85 MPa, which is almost unchanged compared with 2.36 MPa for the neat PU and it can reach even 15.42 MPa for the 70PU/10PLA/0.75CNTs composite (Fig. 3-c). Moreover, it should be noted that the elongation at break of 70PU/10PLA/2CNTs composite is still as high as 1345%, for which significant improvements of the tensile strength at 300% strain (16.15 MPa) and Young's modulus (19.05 MPa) are also observed. This result is apparently different from adding either PLA or CNTs individually, for which the reinforcement is usually not satisfying. In other words, the ternary composites show better mechanical performance compared with the binary counterparts. Particularly, the ternary composites containing a large amount of PLA (30 *wt.*%), 70PU/30PLA/CNTs composites, exhibit superior mechanical properties compared to other composites with less PLA content but the same amounts of CNTs. According to the above results, 70PU/30PLA composites with various contents of CNTs are supposed be the

optimal option to reinforce PU.

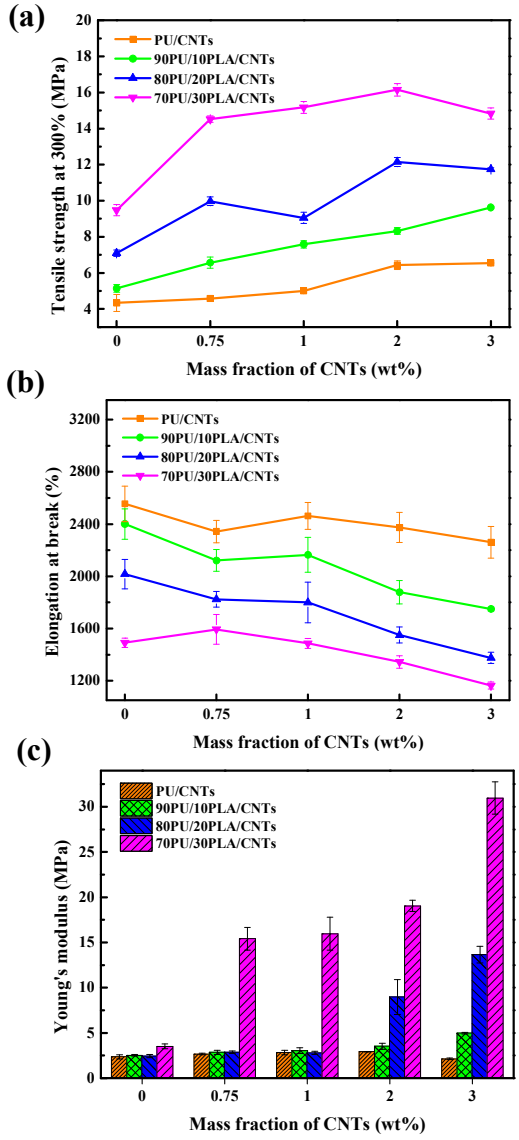


**Fig. 3.** Tensile properties of PU/CNTs composite, 90PU/10PLA/CNTs composite, 80PU/20PLA/CNT composite and 70PU/30PLA/CNTs composite with various contents of CNTs. (a) Tensile strength at 300% strain, (b) Elongation at break and (c) Young's modulus.

### 3.2 Electrical properties of PU/PLA/CNTs composites

It is widely known that CNTs is a kind of prominent modifiers for conductive polymer composites (CPCs) due to its excellent mechanical and physical properties such as high tensile strength, high aspect ratio and excellent electrical conductivity[38-40, 43, 44]. In this work, the electrical conductivities for the PU/CNTs composites, 90PU/10PLA/CNTs composites, 80PU/20PLA/CNTs composites and 70PU/30PLA/CNTs composites with various contents of CNTs are systemically investigated and the results are shown in Fig. 4. As shown in the figure, all the composites show characteristic conductivity trends of CPCs[45, 46]: the electrical conductivity begins with slight increase by the adding of CNTs, followed with sharp increase at a critical CNTs concentration, which refers to the percolation threshold, and then tends to level off. In other words, the percolation threshold is the concentration at which interconnecting conductive networks can be formed in polymer matrix. As shown in Fig. 4, it could be estimated that the percolation threshold is about 2 *wt*.%-2.5 *wt*.% for the composites investigated. With increasing the CNTs content in the PU/CNTs composites from 1 *wt*.% to 3 *wt*.%, the electrical conductivity is found to increase from $1.53\times10^{-6}$ S/m to 0.00941 S/m . As for the 90PU/10PLA/CNTs composites, the electrical conductivity increases significantly from $1.49\times10^{-7}$ S/m to 0.9773 S/m with the CNTs amount increases from 1 *wt*.% to 3 *wt*.%. Moreover, the electrical conductivities remain in the same level for 80PU/20PLA/CNTs and 70PU/30PLA/CNTs composites. The trend of the conductivity properties differs from the mechanical properties, for which the 70PU/30PLA/CNTs composites exhibited better reinforcement than others, indicating that the mechanisms of mechanical reinforcement and conductivity improvement are quite different. It is also worth mentioning that the values of electrical conductivities for the PU/PLA/CNTs composites are even higher than that for the PU/CNTs composites at the same CNTs contents, demonstrating that the ternary composites have better electrical conductivity compared with the binary counterpart.

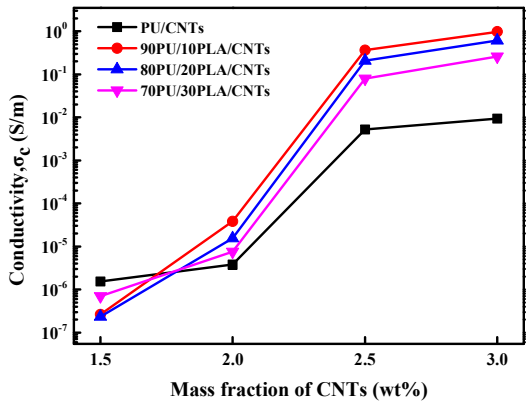


**Fig. 4.** Electrical conductivities of PU/CNTs composites, 90PU/10PLA/CNTs composites, 80PU/20PLA/CNTs composites and 70PU/30PLA/CNTs composites with various contents of CNTs.

### 3.3. Morphology observation

Since the mechanical properties are greatly influenced by both the phase morphologies and the interface adhesion, in order to investigate the mechanisms of mechanical reinforcement and conductivity improvement, the morphologies of the composites and the dispersion of PLA and CNTs were visualized using SEM observations. Fig. 5 shows the overall morphologies for the three kinds of typical samples, *i.e.* PU/CNTs, 90PU/10PLA/CNTs, and 70PU/30PLA/CNTs composites with various contents of CNTs. As shown, CNTs can be well

dispersed in PU matrix and few agglomerates can be observed. The addition of PLA has no effect on the dispersion of CNTs in PU matrix. PLA is uniformly dispersed in PU matrix as spherical particle, but its size increases as increase of its content. The average diameter for the PLA in 90PU/10PLA/CNTs composites is about 0.5 μm, which increases to 1.9 μm for the 70PU/30PLA/CNTs composites. Also the addition of CNTs has no effect on the dispersion of PLA in PU matrix.

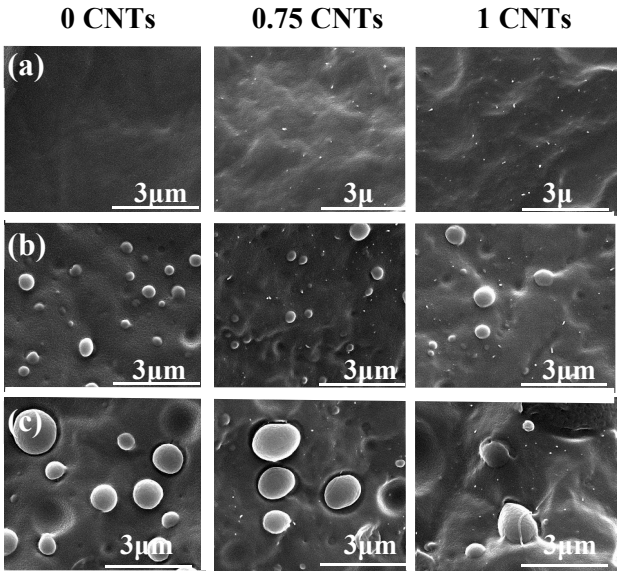


**Fig. 5.** SEM images showing the morphologies of composites with different contents of CNTs. (a) PU/CNTs, (b) 90PU/10PLA/CNTs, and (c) 70PU/30PLA/CNTs.

In order to further analyze the dispersion of CNTs in the composites, SEM images of 70PU/30PLA/1CNTs and 90PU/10PLA/1CNTs at higher magnification are shown in Fig. 6. Interestingly, in the 70PU/30PLA/1CNTs composite, it can be observed that most CNTs are selectively dispersed in the PU matrix and some individual CNTs locate in the interfaces of the continuous PU matrix and the dispersed PLA phase (pointed with red arrows in Fig. 6a), namely, some CNTs exhibit the nano-bridge effect for the immiscible 70PU/30PLA blends. However, as for the 90PU/10PLA/1CNTs composite, no similar nano-bridge distribution of CNTs could be observed. Considering the length of CNTs (1.5 μm) and the different sizes of PLA droplets for 90PU/10PLA/CNTs (0.5 μm) and for 70PU/30PLA/CNTs composites (1.9 μm), the PLA droplets of 90PU/10PLA/CNTs composite might be too small for CNTs to contact. As shown by the red arrows in Fig. 6-b, almost all the CNTs are randomly located in the PU matrix. On the other hand, different from the smooth surface of PLA for the 90PU/10PLA/1CNTs composite, the cryogenically fractured surface of PLA for the 70PU/30PLA/1CNTs composite is rougher, which could be resulted from the nano-bridge CNTs in the interface.

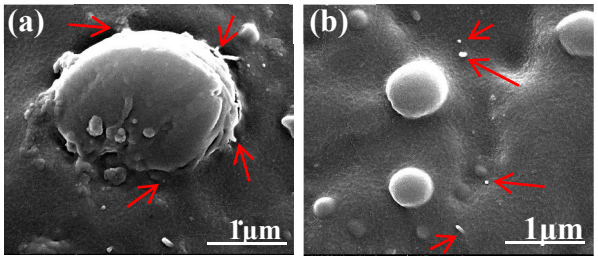


**Fig. 6.** SEM image showing the composite morphologies of (a) 70PU/30PLA/1CNTs and (b) 90PU/10PLA/1CNTs at higher magnification.(The red arrows show the dispersion of CNTs).

In order to confirm this speculation, cryogenically fractured surfaces of the 70PU/30PLA/1CNTs and 90PU/10PLA/1CNTs composites are etched with chloroform to remove PLA and then visualized using SEM. Fig. 7a and Fig. 7b shows the etched fractured surfaces of the 70PU/30PLA/1CNTs composite and the 90PU/10PLA/1CNTs composite at different magnifications, respectively. Obviously, the nano-bridge effect found in Fig. 6a can be further evidenced in Fig. 7a in which CNTs are observed at the boundary of the holes (also shown by red arrows). Similar nano-bridge structure of CNTs has been reported in earlier literatures[37, 43]. For example, in the HDPE/PA 6 system by Xiang et al.[43], such nano-bridge effect improves the interfacial adhesion between HDPE and PA6 composites, facilitating the stress transfer from one phase to the other more efficiently and resulting in the improvement of mechanical strength and the maintain of good ductility. In our work, the SEM images indeed are of low magnification but indeed give some indication that CNTs could be located in the interface of the polymer blends. Since PLA and CNTs are separately dispersed in PU matrix, the distance between CNTs particle and PLA droplet is expected to be decreased with increasing of PLA content or CNTs content. In other words, the big PLA droplets will be easily surrounded by tiny CNTs particles as PLA content is high, and some of CNTs can be located at the interface area. Also the possible CNTs agglomerates at high content are helpful to decrease the distance between CNTs and PLA droplets thus enhance the interaction between PLA and CNTs. Thus the interaction between PU and PLA can be intensified by the CNTs bridge effect, resulting in higher stress transfer efficiency in the composites under the load condition as compared to the blends. Consequently, it is reasonable to conclude that the location of CNTs at the interfaces could cause better tensile strength at 300% strain and Young's modulus in the 70PU/30PLA/CNTs than the 90PU/10PLA/CNTs composites.

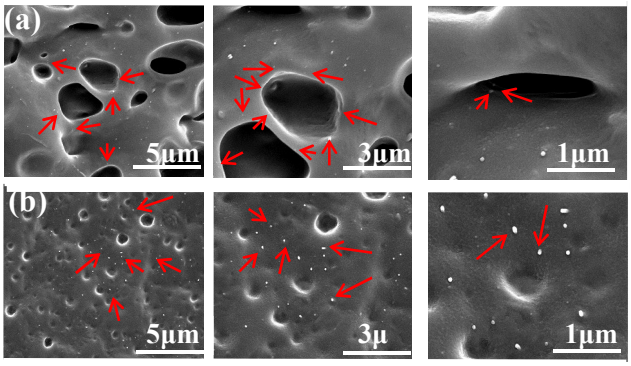


**Fig. 7.** SEM images of the etched fractured surfaces for (a) 70PU/30PLA/1CNTs composite and (b) 90PU/10PLA/1CNTs composite at different magnifications. The surfaces were etched with chloroform to remove PLA. (The red arrows show the dispersion of CNTs).

### 3.4. Rheological analysis

The structure of CNTs network in the composites was further studied using rheological measurement. Fig. 8 shows the storage modulus (G') and complex viscosity (η*). From Fig. 8-a, a slight increase of G' with the increasing content of CNTs can be noticed. For the 100PU/0.75CNTs composite, there is no platform observed in the storage modulus curve at low frequencies. However, for the 70PU/30PLA/0.75CNTs and the 90PU/10PLA/0.75CNTs composites, the storage modulus curve presents a platform at low frequencies. As for the composites with 2 *wt*.% CNTs, all of the three samples exhibit the similar rheological properties that a platform in storage modulus curve at low frequencies is observed. The variations of η* with increasing content of CNTs in the PU/CNTs, 90PU/10PLA/CNTs, and 70PU/30PLA/CNTs composites are shown in Fig. 8-b. The η* increases with the increasing content of CNTs in the composites, which is consist with the result of the storage modulus (G') mentioned before. It has been widely known that the observation of the platform in the storage modulus curve at low frequency is proved to the network structure of a percolated nano-filler in the composites[38]. This phenomenon also indicates the formation of network structures of CNTs in the70PU/30PLA/0.75CNTs and 90PU/10PLA/0.75CNTs composites, in contrast to 100PU/0.75CNTs composite, which could not form the network structure of CNTs. Besides, all of the three composites with the presence of amount (2 *wt*.%) of CNTs exhibit the network structures of CNTs. Nonetheless, this is inconsistent with the mechanical behaviors that the 70PU/30PLA/CNTs composite shows superior mechanical tensile strength and Young's modulus compared to other composites. Thus, it is generally believed that the nano-bridge structure of CNTs and the size increase of PLA particles contribute more efficiently to the improvement of mechanical performances of composites due to the stress transfer from one phase to the other and the network structure mainly attributed to the conductive behavior.

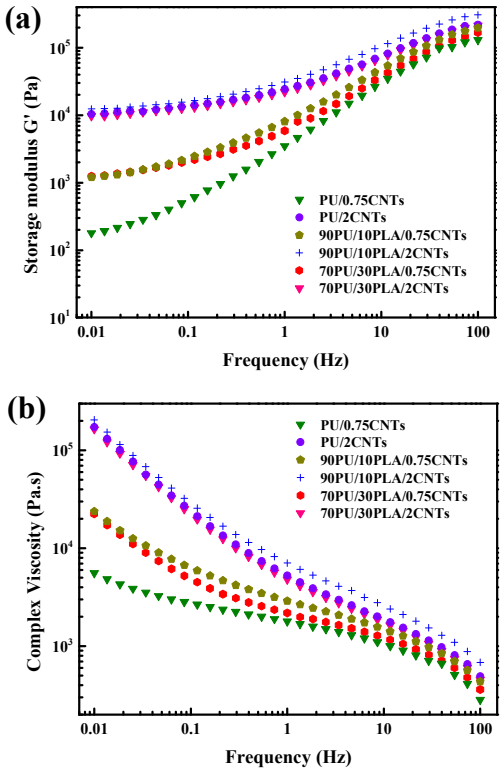


**Fig. 8.** Rheological properties of PU/CNTs composites, 90PU/10PLA/CNTs composites, and 70PU/30PLA/CNTs composites. (a) Storage modulus, (b) complex viscosity.

### 3.5. Understanding about the reinforced mechanical and electrical properties mechanism

To give a more vivid description of the morphologies and to better understand the reinforcement and conductivity mechanism, schematic representations of the 90PU/10PLA/CNTs and 70PU/30PLA/CNTs composites are shown in Fig. 9 according to the above discussions. In the 70PU/30PLA/CNTs composites (as shown in Fig. 9b), PLA is dispersed in the PU matrix as uniform spherical particles with larger size than the 90PU/10PLA/CNTs composite (as shown in Fig. 9a) and some of the individual CNTs locate in the interfaces of the continuous PU matrix and the dispersed PLA phase. However, as for the 90PU/10PLA/1CNTs composites, no similar nano-bridge distribution of CNTs exists. It has been reported that when CNTs are selectively located at the interface of the blends and form the nano-bridge structure, facilitating the stress transfer between components under the load condition, the reinforcement efficiency is much higher compared with which CNTs are selectively located in one component[47-50]. As a consequence, favorable reinforcement without scarifying the ductility could be obtained. Considering the relatively superior mechanical properties of 70PU/30PLA/CNTs composites as compared with 90PU/10PLA/1CNTs composites and the similar electrical conductivities, it can be believed that the

nano-bridge effect of CNTs and the size increase of PLA particles attribute a lot to the improvement of mechanical performances and the network structures of CNTs mainly contributes to the conductive behavior. It should be noted that the formation of interpenetrating network is just a speculation, and need to be proved by more experimental observation. We just tentatively use it to explain the improved mechanical property of the prepared ternary system compared with the binary system.

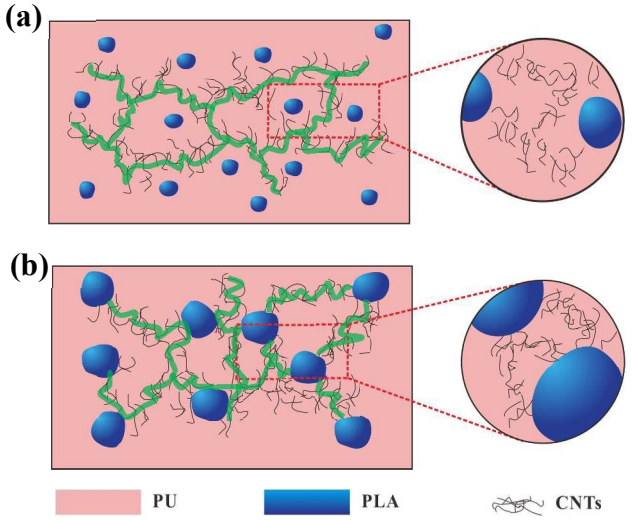


**Fig. 9.** Schematic representation of the composite phase morphology: (a) 90PU/10PLA/CNTs and (b) 70PU/30PLA/CNTs.

## 4. Conclusion

In this paper, we introduced various contents of CNTs into the PU/PLA blends with different weight ratios of PU and PLA via melt blending. The results show that the simultaneously incorporation of PLA and CNTs induces great improvement of mechanical strength and electrical conductivities of PU, which could not be observed in the individual PU/PLA or PU/CNTs composites. Particularly, the ternary composites containing a large amount of PLA (30 *wt*.%), 70PU/30PLA/CNTs composites, exhibit simultaneous superior mechanical properties compared to other composites with less PLA content but the same amounts of CNTs. Moreover, the ternary composites show better electrical conductivity compared with the binary counterpart. Further morphology and rheological results show that both CNTs and PLA are dispersed separately in the PU matrix and tend to contact each other to form well networks, which contribute to the conductive behavior. Moreover, some of the individual CNTs are located in the interfaces, namely, the CNTs exhibit nano-bridge structure in the composites. Such nano-bridge effect and size increase of PLA are believed to improve the mechanical performances of 70PU/30 PLA/CNTs composites.

## Acknowledgements

We express our sincere thanks to the National Natural Science Foundation of China (NNSFC) for financial support (50973065, 51421061).

## Notes and references

*College of Polymer Science and Engineering, State Key Laboratory of Polymer Materials Engineering, Sichuan University, Chengdu 610065, P. R. China. E-mail: qiangfu@scu.edu.cn; bhw_168@163.com; Fax: +86 28 8546 1795; Tel: +86 28 8546 1795*

1. N. M. Lamba, K. A. Woodhouse and S. L. Cooper, *Polyurethanes in biomedical applications*, CRC press, 1997.
2. P. A. Gunatillake, G. F. Meijs, S. J. Mccarthy and R. Adhikari, *J. Appl. Polym. Sci.*, 2000, **76**, 2026-2040.
3. A. Simmons, J. Hyvarinen and L. Poole-Warren, *Biomaterials*, 2006, **27**, 4484-4497.
4. D.-s. Tan, X.-q. Zhang, J.-c. Wang and J.-h. Li, *Chin. J. Polym. Sci.*, 2011, **29**, 615-626.
5. M. S. Kathalewar, P. B. Joshi, A. S. Sabnis and V. C. Malshe, *RSC Advances*, 2013, **3**, 4110-4129.
6. X. Wang, Y.-T. Pan, J.-T. Wan and D.-Y. Wang, *RSC Advances*, 2014, **4**, 46164-46169.
7. P. F. Bruins, *Polyurethane technology*, Wiley-IEEE Press, 1969.
8. Z. S. Petrović and J. Ferguson, *Prog. Polym. Sci.*, 1991, **16**, 695-836.
9. P. Du, X. Liu, Z. Zheng, X. Wang, T. Joncheray and Y. Zhang, *RSC Advances*, 2013, **3**, 15475-15482.
10. A. Bayer, *Edition January, Leverkusen: Bayer-Polyurethanes*, 1979.
11. B. S. Chiou and P. E. Schoen, *J. Appl. Polym. Sci.*, 2002, **83**, 212-223.
12. Z. Wirpsza, *Polyurethanes: chemistry, technology, and applications*, Ellis Horwood, 1993.
13. S. Thakur and N. Karak, *Rsc Advances*, 2013, **3**, 9476-9482.
14. J. Zhu, S. Wei, I. Y. Lee, S. Park, J. Willis, N. Haldolaarachchige, D. P. Young, Z. Luo and Z. Guo, *Rsc Advances*, 2012, **2**, 1136-1143.
15. J. Ge, Y. Si, F. Fu, J. Wang, J. Yang, L. Cui, B. Ding, J. Yu and G. Sun, *RSC Advances*, 2013, **3**, 2248-2255.
16. X. Wang, B. Mu and H. Wang, *Polym. Compos.*, 2014.
17. H. Hong, J. Wei, Y. Yuan, F. P. Chen, J. Wang, X. Qu and C. S. Liu, *J. Appl. Polym. Sci.*, 2011, **121**, 855-861.
18. T. Chen, Y. Tien and K. Wei, *J J. Polym. Sci., Part A: Polym. Chem.*, 1999, **37**, 2225-2233.
19. S. L. Zhang, G. B. Wang, Z. H. Jiang, W. C. Wu, R. T. Ma and Z. W. Wu, *J. Appl. Polym. Sci.*, 2004, **94**, 839-844.
20. S. L. Zhang, G. B. Wang, Z. H. Jiang, D. Wang, R. T. Ma and Z. W. Wu, *J. Polym. Sci., Part B: Polym. Phys.*, 2005, **43**, 1177-1185.
21. W. Chen, X. Tao and Y. Liu, *Compos. Sci. Technol.*, 2006, **66**, 3029-3034.
22. N. G. Sahoo, Y. C. Jung, H. J. Yoo and J. W. Cho, *Macromol. Chem. Phys.*, 2006, **207**, 1773-1780.
23. W. Zhang, N. Ning, Y. Gao, F. Xu and Q. Fu, *Compos. Sci. Technol.*, 2013, **83**, 47-53.
24. L. Yang, S. L. Phua, C. L. Toh, L. Zhang, H. Ling, M. Chang, D. Zhou, Y. Dong and X. Lu, *RSC Advances*, 2013, **3**, 6377-6385.

25. D. A. Nguyen, Y. R. Lee, A. V. Raghu, H. M. Jeong, C. M. Shin and B. K. Kim, *Polym. Int.*, 2009, **58**, 412-417.
26. Z. S. Petrović, I. Javni, A. Waddon and G. Bánhegyi, *J. Appl. Polym. Sci.*, 2000, **76**, 133-151.
27. T. Cotgreave and J. Shortall, *J. Mater. Sci.*, 1977, **12**, 708-717.
28. Q. Wu, M. Henriksson, X. Liu and L. A. Berglund, *Biomacromolecules*, 2007, **8**, 3687-3692.
29. A. Pei, J.-M. Malho, J. Ruokolainen, Q. Zhou and L. A. Berglund, *Macromolecules*, 2011, **44**, 4422-4427.
30. C.-z. Geng, X. Hu, G.-h. Yang, Q. Zhang and F. Chen, *Chin. J. Polym. Sci.*, 2015, **33**, 61-69.
31. Z. Wang and T. J. Pinnavaia, *Chem. Mater.*, 1998, **10**, 3769-3771.
32. G. Yang, C. Geng, J. Su, W. Yao, Q. Zhang and Q. Fu, *Compos. Sci. Technol.*, 2013, **87**, 196-203.
33. N. Najafi, M. Heuzey and P. Carreau, *Compos. Sci. Technol.*, 2012, **72**, 608-615.
34. E. d. M. Teixeira, A. De Campos, J. Marconcini, T. Bondancia, D. Wood, A. Klamczynski, L. Mattoso and G. Glenn, *RSC Advances*, 2014, **4**, 6616-6623.
35. S. Peng, P. Zhu, Y. Wu, S. G. Mhaisalkar and S. Ramakrishna, *Rsc Advances*, 2012, **2**, 652-657.
36. M. Yao, H. Deng, F. Mai, K. Wang, Q. Zhang, F. Chen and Q. Fu, *Express Polym. Lett.*, 2011, **5**, 937.
37. C. Zeng, N. Hossieny, C. Zhang, B. Wang and S. M. Walsh, *Compos. Sci. Technol.*, 2013, **82**, 29-37.
38. H. D. Wagner, P. Ajayan and K. Schulte, *Compos. Sci. Technol.*, 2013, **83**, 27-31.
39. J. Chen, X.-C. Du, W.-B. Zhang, J.-H. Yang, N. Zhang, T. Huang and Y. Wang, *Compos. Sci. Technol.*, 2013, **81**, 1-8.
40. M. Mohiuddin and S. V. Hoa, *Compos. Sci. Technol.*, 2013, **79**, 42-48.
41. Y. Gao, G.-y. Zong and H.-w. Bai, *Chin. J. Polym. Sci.*, 2014, **32**, 245-254.
42. J. Zhu, J. Jiang, J. Liu, R. Ding, Y. Li, H. Ding, Y. Feng, G. Wei and X. Huang, *Rsc Advances*, 2011, **1**, 1020-1025.
43. X. Gao, C. Qu, Q. Zhang, Y. Peng and Q. Fu, *Macromol. Mater. Eng.*, 2004, **289**, 41-48.
44. H. Xiu, Y. Zhou, J. Dai, C. Huang, H. Bai, Q. Zhang and Q. Fu, *RSC Advances*, 2014, **4**, 37193-37196.
45. H. Deng, L. Lin, M. Ji, S. Zhang, M. Yang and Q. Fu, *Prog. Polym. Sci.*, 2014, **39**, 627-655.
46. H. Pang, Y.-Y. Piao, L. Xu, Y. Bao, C.-H. Cui, Q. Fu and Z.-M. Li, *RSC Advances*, 2013, **3**, 19802-19806.
47. F. Xiang, J. Wu, L. Liu, T. Huang, Y. Wang, C. Chen, Y. Peng, C. Jiang and Z. Zhou, *Polym. Advan. Technol.*, 2011, **22**, 2533-2542.
48. Y. Shi, Y. Li, F. Xiang, T. Huang, C. Chen, Y. Peng and Y. Wang, *Polym. Advan. Technol.*, 2012, **23**, 783-790.
49. J. Chen, Y.-y. Shi, J.-h. Yang, N. Zhang, T. Huang and Y. Wang, *Polymer*, 2013, **54**, 464-471.
50. Y.-h. Wang, X.-l. Xu, J. Dai, J.-h. Yang, T. Huang, N. Zhang, Y. Wang, Z.-w. Zhou and J.-h. Zhang, *RSC Advances*, 2014, **4**, 59194-59203.



 